

Figure 5. The influence of Cadm1 deficiency on the expression of synaptic proteins and Foxp2 in the cerebellum. (A) Immunoblot analysis of the influence of the deficiency in the cerebellums of *Cadm1* KO and wild-type pups (P10). An example of the typical immunoblotting results is shown. Values are mean±standard error (SEM). Student's *t*-test (* $p < 0.05$, ** $p < 0.01$). Pups: $n = 5$. All experiments were performed three times. (B) RT-PCR analysis of the influence of the *Cadm1* deficiency on the expression of *Foxp2* in the cerebellum of wild-type and *Cadm1* KO pups (P10). Values are mean±standard error (SEM). Pups: $n = 5$. All experiments were performed three times. A comparison showed no significant difference (Student's *t*-test; $p < 0.05$).
doi:10.1371/journal.pone.0030151.g005

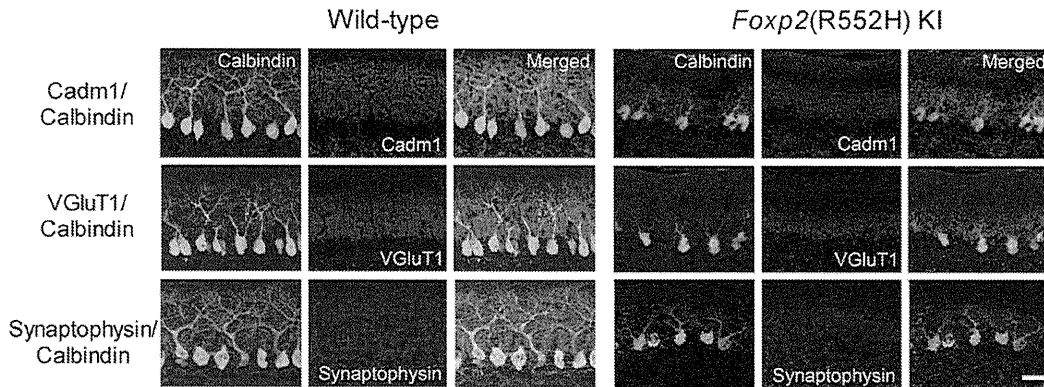


Figure 6. Altered distribution of Cadm1 in the molecular layer of wild-type and *Foxp2*(R552H) KI mice (P11). Cadm1 preferentially distributed in the apical-distal dendritic portion in the molecular layer. The immunoreactivity of Cadm1 as well as that of Synaptophysin and VGluT1, pre-synaptic markers, was decreased in the molecular layer of the *Foxp2*(R552H) KI mice. Green, Calbindin. Red, Cadm1, VGluT1, Synaptophysin. Blue, Hoechst. Bar, 30 μm .
doi:10.1371/journal.pone.0030151.g006

animals per genotype were examined, and experiments were repeated three times. Quantification of staining intensities was done using LAS AF software (Leica Microsystems). The mean pixel value in the area of interest and in the same size area of the background was calculated. The background level was subtracted from the value found in the area of interest (in the molecular layer). Reported intensities were normalized to control, and the Student's *t*-test was performed for statistical analysis.

Supporting Information

Figure S1 Alteration of Purkinje cells in cerebellum of wild-type and *Foxp2*(R552H) knock-in (*Foxp2* KI) mice, wild-type, and *Cadm1* knockout (*Cadm1* KO) (P11). The immunoreactivity was performed using mouse anti-Calbindin. Bar, 20 μm . (TIF)

Figure S2 Altered distribution of the Cadm1 of wild-type and *Foxp2*(R552H) KI mice (P11). Values are mean±

standard error (SEM). Student's *t*-test (** $p < 0.01$). Pups: $n = 3$. Images: $n = 10$. (TIF)

Figure S3 RT-PCR analysis of the expression of *Cadm1* in the cerebellum of wild-type and *Foxp2*(R552H) KI mice (P10). Values are mean±standard error (SEM). Pups: $n = 5$. All experiments were performed three times. A comparison showed no significant difference (Student's *t*-test; $p < 0.05$). (TIF)

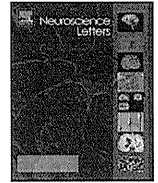
Figure S4 The immunoreactivity (p11) of Synaptophysin (pre-synaptic marker) and PSD-95 (post-synaptic marker). Green, Cadm1. Red, Synaptophysin or PSD-95 (Cell Signaling Technology). Blue, Hoechst. Bar, 30 μm . (TIF)

Author Contributions

Conceived and designed the experiments: TM MYM BI. Performed the experiments: EF YT. Analyzed the data: EF TM. Contributed reagents/materials/analysis tools: EF TM. Wrote the paper: EF BI TM.

References

- Biederer T, Sara Y, Mozhayeva M, Atasoy D, Liu X, et al. (2002) SynCAM, a synaptic adhesion molecule that drives synapse assembly. *Science* 297: 1525–1531.
- Fujita E, Soyama A, Momoi T (2003) RA175, which is the mouse ortholog of TSLC1, a tumor suppressor gene in human lung cancer, is a cell adhesion molecule. *Exp Cell Res* 287: 57–66.
- Jamain S, Quach H, Betancur C, Råstam M, Colineaux C, et al. (2003) Mutations of the X-linked genes encoding neuroligins NLGN3 and NLGN4 are associated with autism. *Nat Genet* 34: 27–29.
- Bakkaloglu B, O'Roak BJ, Louvi A, Gupta AR, Abelson JF, et al. (2008) Molecular cytogenetic analysis and resequencing of contactin associated protein-like 2 in autism spectrum disorders. *Am J Hum Genet* 82: 165–173.
- Zhiling Y, Fujita E, Tanabe Y, Yamagata T, Momoi T, et al. (2008) Mutations in the gene encoding CADM1 are associated with autism spectrum disorder. *Biochem Biophys Res Commun* 377: 926–929.
- Fujita E, Dai H, Tanabe Y, Zhiling Y, Yamagata T, et al. (2010) Autism Spectrum Disorder is related to endoplasmic reticulum stress induced by mutations in the synaptic cell adhesion molecule, CADM1. *Cell death disease* 1: e47.
- Fujita E, Kouroku Y, Ozeki S, Tanabe Y, Toyama Y, et al. (2006) Oligoastheno-teratozoospermia in mice lacking RA175/TSLC1/SynCAM/IGSF4A, a cell adhesion molecule in the immunoglobulin superfamily. *Mol Cell Biol* 26: 718–726.
- Takayanagi Y, Fujita E, Yu Z, Yamagata T, Momoi MY, et al. (2010) Impairment of social and emotional behaviors in Cadml-knockout mice. *Biochem Biophys Res Commun* 396: 703–708.
- Lai CS, Fisher SE, Hurst JA, Vargha-Khadem F, Monaco AP (2001) A forkhead-domain gene is mutated in a severe speech and language disorder. *Nature* 413: 519–523.
- Li S, Weidenfeld J, Morrisey EE (2004) Transcriptional and DNA binding activity of the Foxp1/2/4 family is modulated by heterotypic and homotypic protein interactions. *Mol Cell Biol* 24: 809–822.
- Vernes SC, Newbury DF, Abrahams BS, Winchester L, Nicod J, et al. (2008) A functional genetic link between distinct developmental language disorders. *N Engl J Med* 359: 2337–2345.
- Branchi I, Santucci D, Alleva E (2001) Ultrasonic vocalisation emitted by infant rodents: a tool for assessment of neurobehavioural development. *Behav Brain Res* 125: 49–56.
- Fujita E, Tanabe Y, Shiota A, Ueda M, Suwa K, et al. (2008) Ultrasonic vocalization impairment of Foxp2 (R552H) knockin mice related to speech-language disorder and abnormality of Purkinje cells. *Proc Natl Acad Sci USA* 105: 3117–3122.
- Shu W, Cho JY, Jiang Y, Zhang M, Weisz D, et al. (2005) Altered ultrasonic vocalization in mice with a disruption in the Foxp2 gene. *Proc Natl Acad Sci USA* 102: 9643–9648.
- Ritvo ER, Freeman BJ, Scheibel AB, Duong T, Robinson H, et al. (1986) Lower Purkinje cell counts in the cerebella of four autistic subjects: initial findings of the UCLA-NSAC Autopsy Research Report. *Am J Psychiatry* 143: 862–866.
- Urase K, Soyama A, Fujita E, Momoi T (2001) Expression of RA175 mRNA, a new member of the immunoglobulin superfamily, in developing mouse brain. *Neuroreport* 12: 3217–3221.
- Fujita E, Urase K, Soyama A, Kouroku Y, Momoi T (2005) Distribution of RA175/TSLC1/SynCAM, a member of the immunoglobulin superfamily, in the developing nervous system. *Brain Res Dev Brain Res* 154: 199–209.
- Miyazaki T, Fukaya M, Shimizu H, Watanabe M (2003) Subtype switching of vesicular glutamate transporters at parallel fibre-Purkinje cell synapses in developing mouse cerebellum. *Eur J Neurosci* 17: 2563–2572.
- Boulland JL, Qureshi T, Seal RP, Rafiki A, Gundersen V, et al. (2004) Expression of the vesicular glutamate transporters during development indicates the widespread corelease of multiple neurotransmitters. *J Comp Neurol* 480: 264–280.
- Xue G, Dong Q, Jin Z, Chen C (2004) Mapping of verbal working memory in nonfluent Chinese-English bilinguals with functional MRI. *Neuroimage* 22: 1–10.
- Dietrich S, Hertrich I, Alter K, Ischebeck A, Ackermann H (2008) Understanding the emotional expression of verbal interjections: a functional MRI study. *Neuroreport* 19: 1751–1755.
- Robbins EM, Krupp AJ, Perez de Arce K, Ghosh AK, Fogel AI, et al. (2010) SynCAM 1 adhesion dynamically regulates synapse number and impacts plasticity and learning. *Neuron* 68: 894–906.
- Newbury DF, Monaco AP (2010) Genetic advances in the study of speech and language disorders. *Neuron* 68: 309–320.
- Fujita E, Tanabe Y, Hirose T, Aurrand-Lions M, Kasahara T, et al. (2007) Loss of partitioning-defective-3/isotype-specific interacting protein (par-3/ASIP) in the elongating spermatid of RA175 (IGSF4A/SynCAM)-deficient mice. *Am J Pathol* 171: 1800–1810.



Cntnap2 expression in the cerebellum of *Foxp2*(R552H) mice, with a mutation related to speech-language disorder

Eriko Fujita^{a,b}, Yuko Tanabe^a, Mariko Y. Momoi^b, Takashi Momoi^{a,*}

^a Center for Medical Science, International University of Health and Welfare, 2600-1, Kitakanemaru, Ohtawara, Tochigi, Japan

^b Department of Pediatrics, Jichi Medical University, 3311-1 Yakushiji, Shimotsukeshi, Tochigi 329-0498, Japan

ARTICLE INFO

Article history:

Received 23 July 2011

Received in revised form 5 November 2011

Accepted 13 November 2011

Keywords:

Foxp2

CtBP

Speech-language

Cntnap2

ABSTRACT

Foxp2(R552H) knock-in (KI) mice carrying a mutation related to human speech-language disorder exhibit impaired ultrasonic vocalization and poor Purkinje cell development. *Foxp2* is a forkhead domain-containing transcriptional repressor that associates with its co-repressor CtBP; *Foxp2*(R552H) displays reduced DNA binding activity. A genetic connection between *FOXP2* and *CNTNAP2* has been demonstrated *in vitro*, but not *in vivo*. Here we show that *Cntnap2* mRNA levels significantly increased in the cerebellum of *Foxp2*(R552H) KI pups, although the cerebellar population of *Foxp2*-positive Purkinje cells was very small. Furthermore, *Cntnap2* immunofluorescence did not decrease in the poorly developed Purkinje cells of *Foxp2*(R552H) KI pups, although synaptophysin immunofluorescence decreased. *Cntnap2* and CtBP were ubiquitously expressed, while *Foxp2* co-localized with CtBP only in Purkinje cells. Taken together, these observations suggest that *Foxp2* may regulate ultrasonic vocalization by associating with CtBP in Purkinje cells; *Cntnap2* may be a target of this co-repressor.

© 2011 Elsevier Ireland Ltd. All rights reserved.

1. Introduction

Autism spectrum disorder (ASD) is one of the most heritable neurodevelopmental disorders [22]. Mutations in the genes encoding contactin-associated protein 2 (*CNTNAP2* and *Caspr2*) have been identified in patients with ASD and impaired speech-language [2,3]. On the other hand, *FOXP2*, a forkhead box-containing gene, is the causative gene of speech-language disorder [17]; the missense mutation *FOXP2* (R553H) co-segregates with members of the KE family affected with speech-language disorder.

Cntnap2 is an adhesion molecule required for the formation of axoglial paranodal junctions surrounding the nodes of Ranvier in myelinated axons [21,23]. In the human brain, *CNTNAP2* is also expressed in the circuits important for language development [2]. *Cntnap2* is localized to the synaptic plasma membrane fraction [3] and to membrane traffic vesicles [4,20]. The C-terminal region of *Cntnap2* contains the PDZ binding domain EYFI [14], which is similar to that of *Cadm1*, a synaptic adhesion molecule related to ASD [11,19,26]. *Cntnap2* associates in *cis* with the contactin family, the glycosyl-phosphatidyl inositol-anchored neural cell adhesion molecule contactin/F3, TAG-1, NB-1, and NB-2, molecules required

for the transport of *Cntnap2* to the cell surface [9]. *Cntnap2* also acts as a negative regulator of neurite outgrowth [8].

The relationship between speech-language disorder and ASD is not clear, although impaired social communication, including speech-language, is one of the phenotypes of ASD patients. *FOXP2* has DNA-binding activity and exhibits repressor activity via its interaction with co-repressors such as C-terminal binding protein (CtBP) [18]. A genetic connection between *FOXP2* and *CNTNAP2* has been shown *in vitro* [25]; *FOXP2* binds the CAAATT motif in an intron of *CNTNAP2* and negatively regulates the expression of *CNTNAP2* mRNA, but *FOXP2*(R553H) does not.

Infant rodents emit ultrasonic vocalizations (USVs), whistle-like sounds of frequencies between 40 and 100 kHz, that play an important communicative role in mother–offspring interactions when the pups are isolated from their mother and littermates [5]. *Foxp2* knock-out (KO) pups and knock-in (KI) pups harboring the *Foxp2*(R552H) mutation that corresponds to the human *FOXP2*(R553H) mutation exhibit severe USV impairment, suggesting that human speech and mouse USVs have a common molecular basis in the brain [15,24]. *Foxp2*(R552H) KI mice also display poor Purkinje cell development in the cerebellum [15]. Microarray analysis of the cerebellar gene expression of *Foxp2*(R552H) KI pups (P10) suggests that *Foxp2* regulates USV-related gene expression in Purkinje cells.

To provide additional insight into the relationship between impairment of speech-language and ASD, we examined co-localization of CtBP and *Foxp2* as well as *Cntnap2* expression in the cerebellum of *Foxp2*(R552H) KI mice with impaired USV. Our

Abbreviations: *Cntnap2*, contactin-associated protein 2; CtBP, C-terminal binding protein; USV, ultrasonic vocalization; ASD, autism spectrum disorder.

* Corresponding author. Tel.: +81 287 24 3162; fax: +81 287 24 3162.

E-mail address: momoi@iuhw.ac.jp (T. Momoi).

observations demonstrate the *in vivo* genetic connection between *Foxp2* and *Cntnap2*.

2. Materials and methods

We followed the fundamental guidelines for proper conduct of animal experiment and related activities in Academic Research Institutions under the jurisdiction of the Ministry of Education, Culture, Sports, Science and Technology, and all of the protocols for animal handling and treatment were reviewed and approved by the Animal Care and Use Committee of Jichi University (approval numbers, H22-179; 10-179) and International University of Health and Welfare (approval numbers, D1008; 10118). Wild-type and *Foxp2*(R552H) KI mice (129/sv) [15] (male mice) were used for experiments.

Mouse brains were fixed in 4% paraformaldehyde in phosphate buffered saline (PBS) at 4°C overnight. Frozen sections (10 µm thick) were cut on a cryostat and immunostained with mouse anti-calbindin (Sigma), rabbit anti-calbindin (Sigma), mouse anti-synaptophysin (Sigma), mouse anti-CTBP (Santa Cruz Biotech.), rabbit anti-caspr2 (*Cntnap2*; Abcam), and rabbit anti-*Foxp2* (Abcam). Alexa Fluor 488 and Alexa Fluor 568 conjugated secondary antibodies against mouse and rabbit IgG were purchased from Molecular Probes. Nuclei were detected by Hoechst 33342 (Molecular Probes). The reactivity was viewed using a Leica AF6000 immunofluorescence microscope or a Leica SP5 confocal microscope (Leica Microsystems). At least three different animals per genotype and experiments were repeated three times.

Total RNA was prepared from brains of wild-type and *Cadm1* KO [13] and *Foxp2*(R552H) KI male mice [15] by RNeasy mini kit (Qiagen) according to the manufacturer's specifications. Complementary DNAs were synthesized from total RNA (1 µg) using reverse transcriptase (Invitrogen) as described previously [12]. Quantitative real-time (RT) PCR analysis was performed by Applied Biosystems 7500 fast real-time PCR system (Applied Biosystems) using the TaqMan Gene Expression Assays (Applied Biosystems) based on published sequences for genes encoding the respective mouse *Cntnap2*, and VIC-labeled mouse *Gapd* (VIC-labeled MGD probe; Applied Biosystems) as endogenous control. For each sample, the 20 µl total volume consisted of 10 µl TaqMan Fast Universal PCR Master Mix (2×; Applied Biosystems), 1 µl TaqMan Gene Expression Assays, and 5 µl of each first-strand cDNA sample. The real-time PCR fragments were amplified as follows: 1 cycle at 95 °C

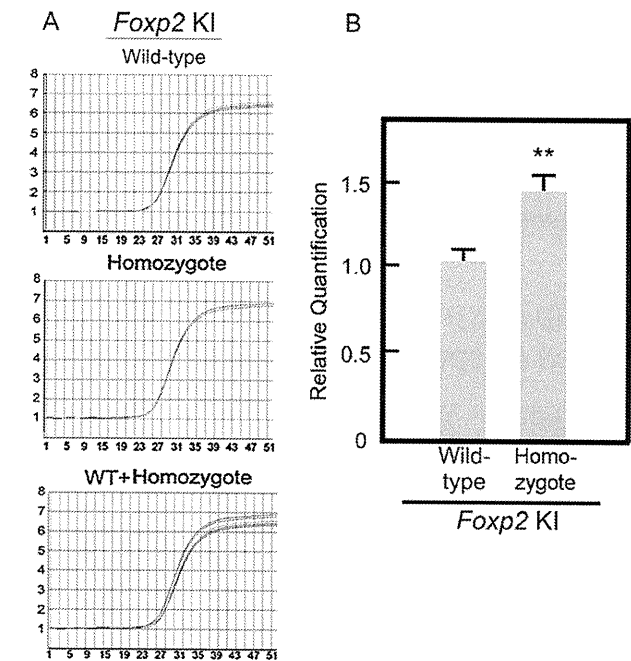


Fig. 1. Increased expression of *Cntnap2* in the cerebellum of *Foxp2*(R552H) KI mice (P10). Quantitative real-time PCR analysis of the expression of *Cntnap2* mRNA in the cerebellum of *Foxp2*(R552H) KI mice (A and B). The expression of *Cntnap2* mRNA in *Foxp2*(R552H) KI mice was compared with that in wild-type mice. Values are mean \pm SEM for at least three independent determinations. Student's *t*-test (** $p < 0.01$).

for 20 s, 60 cycles at 95 °C for 3 s and 60 °C for 30 s. Results were analysed by Student's *t*-test ($p < 0.05$ was considered statistically significant).

3. Results

We quantitatively measured the level of *Cntnap2* mRNA in the cerebella of wild-type and *Foxp2*(R552H) KI pups (P10). The level of *Cntnap2* mRNA increased 1.6-fold ($p < 0.05$) in the cerebellum of *Foxp2*(R552H) KI mice (Fig. 1A and B). However, the mRNA levels of other genes, including *Cadm1*, were unchanged (Supplementary Fig. S1). Thus, the expression of *Cntnap2* appears to be under the control of *Foxp2* in the cerebellum.

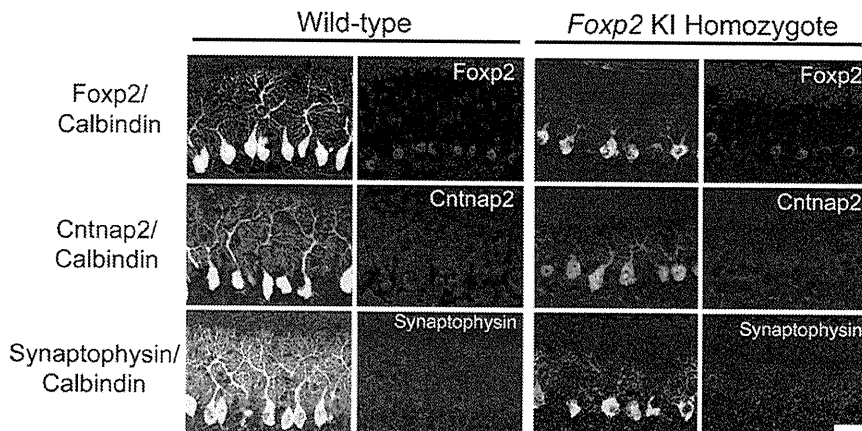


Fig. 2. *Cntnap2* localization in the cerebellum of *Foxp2*(R552H) KI pups. *Cntnap2* distribution was examined in the cerebellum of wild-type and *Foxp2*(R552H) KI pups (P10) by immunostaining. The *Cntnap2* intensity preferentially distributed in the proximal dendritic portion. In contrast with synaptophysin, intensity of *Cntnap2* immunoreactivity was not decreased in the *Foxp2*(R552H) KI pups. Green; calbindin. Red; *Foxp2*, *Cntnap2* or synaptophysin. Blue; Hoechst. Bar indicates 30 µm.

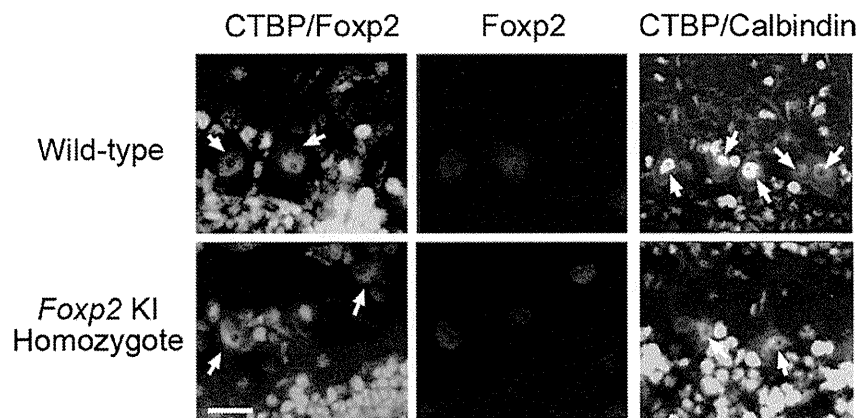


Fig. 3. Localization and distribution of CtBP in the cerebellum of wild-type and *Foxp2*(R552H) KI mice (P10). The CtBP co-localized with Foxp2 (left panel). The CtBP localized both in the Purkinje cells and granular cells (right panel). As Foxp2 localized in the nuclei of Purkinje cells (see Fig. 2), the CtBP co-localized with Foxp2 in the nuclei of Purkinje cells. Green; CtBP. Red; Foxp2 or calbindin. Blue; Hoechst. Bar indicates 30 μ m.

To elucidate the role of *Cntnap2* in USV, we examined *Cntnap2* localization in the cerebella of wild-type and *Foxp2*(R552H) KI mice. *Cntnap2* immunoreactivity was preferentially located in the soma and proximal dendritic portion of Purkinje cells, as well as in the granular cells of the wild-type P10 pups (Fig. 2). *Foxp2*(R552H) KI pups exhibited poor development of Purkinje cell dendrites with reduced synaptophysin immunoreactivity [15]. In contrast, the intensity of *Cntnap2* immunofluorescence was apparently unchanged (Fig. 2). However, given the poor development and decreased number (20% reduction) of Purkinje cells in the *Foxp2*(R552H) KI pups, the intensity of *Cntnap2* immunofluorescence seems to be relatively increased in the Purkinje cells.

Foxp2 associates with its co-repressor CtBP and acts as a transcriptional repressor [18]. In the cerebellum, CtBP localized to the nuclei of granular cells and Purkinje cells (Fig. 3, right), while Foxp2 localized to the nuclei of Purkinje cells but not granular cells (Fig. 2). CtBP co-localized with Foxp2 and *Foxp2*(R552H) in the Purkinje cells of wild-type and *Foxp2*(R552H) KI mice, respectively (Fig. 3, left).

4. Discussion

Foxp2(R552H) KI mice exhibit abnormal cerebellar development and poor dendrite development [15]. In addition, the selective expression of FOXP2 in the Purkinje cells of *Foxp2*(R552H) KI mice partially improves their USVs (unpublished observation), suggesting that Purkinje cells are an essential component of the Foxp2-mediated USV network. We observed a statistically significant increase in *Cntnap2* mRNA levels in *Foxp2*(R552H) KI mice. Expression of *Cntnap2* and its co-repressor CtBP was ubiquitous in granular cells and Purkinje cells, but Foxp2 expression was restricted to the Purkinje cells. Given the ratio of granular cells to Purkinje cells in the cerebellum, *Cntnap2* mRNA must be up-regulated in the Purkinje cells of the *Foxp2*(R552H) KI mice more than 1.6 fold. Thus, our observations suggest that *Cntnap2* is a Foxp2 target in Purkinje cells, and that the Foxp2 and CtBP complex acts as a transcriptional repressor.

The apparently unchanged intensity of *Cntnap2* immunofluorescence in *Foxp2*(R552H) KI mice, which display poor Purkinje cell dendrite development and decreased synaptophysin immunofluorescence, suggests that *Cntnap2* expression is relatively increased in the decreased number of synapses on the dendrites. *Cntnap2* must be up-regulated and degraded, whereas synaptophysin may not be up-regulated but is degraded.

Human speech and mouse USVs have a common molecular basis in the brain that is mediated by Foxp2 [15,24], and the cerebellum is related to the network engaged in the production of spoken human language [1,6]. Functional magnetic resonance imaging has suggested the existence of two cerebrocerebellar networks for human verbal working memory; cerebellar abnormality with Purkinje cell loss has been observed in several autopsy samples from ASD patients [10]. A *Cntnap2* mutation occurs in ASD patients with speech-language disorder [2,3], suggesting that *Cntnap2* is an essential factor for speech-language. However, *Cntnap2* is relatively up-regulated in the Purkinje cells of *Foxp2*(R552H) KI pups (Fig. 1) with impaired USV. *Cntnap2* is a negative regulator of neurite outgrowth [8], suggesting that *Cntnap2* may be a negative regulator in the network involved in Foxp2-mediated USV and/or speech-language. However, it is presently unclear why *Cntnap2*-mediated negative regulation is necessary for Foxp2-mediated USV. This unresolved question will be an important issue for future study; USV and speech-language function may be regulated by a dual positive and negative synaptic system.

Cntnap2 may cooperate or compete with synaptic adhesion molecules, including *Cadm1*, in Foxp2-mediated USV. Mutations in *CADM1* and *NLGN-3* occur in ASD patients [7,26]. *Cadm1* KO, as well as *Nlgn-3*- and *Nlgn-4*-deficient mice, exhibit impaired USV [16], and *Cadm1* localizes to the molecular layer of the dendritic arbor of Purkinje cells, with reduced distribution in *Foxp2*(R552H) KI pups (Fujita et al., submitted). *Cntnap2* localized not only to the proximal dendrites, but also to the soma of Purkinje cells (Fig. 2) and to membrane traffic vesicles [4,20], indicating that *Cntnap2* is involved in the membrane trafficking of synaptic molecules to the synapse. Since the cytoplasmic tail of *Cntnap2* carries a PDZ binding motif identical to the one in *Cadm1*, and since its *cis*-binding partners are members of the contactin family of the immunoglobulin superfamily, it may be possible that the contactin-2(TAG-1)-*Cntnap2* complex and *Cadm1* cooperatively or competitively participate in speech-language and USV activity in the molecular layer.

In conclusion, *Cntnap2* expression is repressed by Foxp2 in Purkinje cells. *Cntnap2* may cooperate or compete with synaptic molecules such as *Cadm1* in Foxp2-mediated USV and speech-language.

Conflict of interest

The authors declare no conflict of interest.

Acknowledgements

This work was supported by Grants-in-Aid for Scientific Research (KAKENHI) of the Ministry of Education, Culture, Sports, Science and Technology, Japan (21200011, 21700377); Grants-in-Aid for Health Labour Scientific Research of the Ministry of the Health, Labour and Welfare, Japan (10103243).

Appendix A. Supplementary data

Supplementary data associated with this article can be found, in the online version, at doi:10.1016/j.neulet.2011.11.022.

References

- [1] H. Ackermann, Cerebellar contributions to speech production and speech perception: psycholinguistic and neurobiological perspectives, *Trends Neurosci.* 31 (2008) 265–272.
- [2] M. Alarcon, B.S. Abrahams, J.L. Stone, J.A. Duvall, J.V. Perederiy, J.M. Bomar, J. Sebat, M. Wigler, C.L. Martin, D.H. Ledbetter, S.F. Nelson, R.M. Cantor, D.H. Geschwind, Linkage, association, and gene-expression analyses identify CNTNAP2 as an autism-susceptibility gene, *Am. J. Hum. Genet.* 82 (2008) 150–159.
- [3] B. Bakkaloglu, B.J. O'Roak, A. Louvi, A.R. Gupta, J.F. Abelson, T.M. Morgan, K. Chawarska, A. Klin, A.G. Ercan-Sencice, A.A. Stillman, G. Tanriover, B.S. Abrahams, J.A. Duvall, E.M. Robbins, D.H. Geschwind, T. Biederer, M. Gunel, R.P. Lifton, M.W. State, Molecular cytogenetic analysis and resequencing of contactin associated protein-like 2 in autism spectrum disorders, *Am. J. Hum. Genet.* 82 (2008) 165–173.
- [4] C. Bel, K. Oguievetskaia, C. Pitaval, L. Goutebroze, C. Faivre-Sarrailh, Axonal targeting of Caspr2 in hippocampal neurons via selective somatodendritic endocytosis, *J. Cell Sci.* 122 (2009) 3403–3413.
- [5] I. Branchi, D. Santucci, E. Alleva, Ultrasonic vocalisation emitted by infant rodents: a tool for assessment of neurobehavioural development, *Behav. Brain Res.* 125 (2001) 49–56.
- [6] S.H. Chen, J.E. Desmond, Cerebrocerebellar networks during articulatory rehearsal and verbal working memory tasks, *Neuroimage* 24 (2005) 332–338.
- [7] D. Comoletti, A. De Jaco, L.L. Jennings, R.E. Flynn, C. Gaietta, I. Tsigelny, M.H. Ellisman, P. Taylor, The Arg451Cys-neurexin-3 mutation associated with autism reveals a defect in protein processing, *J. Neurosci.* 24 (2004) 4889–4893.
- [8] V. Devanathan, I. Jakovcevski, A. Santucci, S. Li, H.J. Lee, E. Peles, I. Leshchynska, V. Sytnyk, M. Schachner, Cellular form of prion protein inhibits Reelin-mediated shedding of Caspr from the neuronal cell surface to potentiate Caspr-mediated inhibition of neurite outgrowth, *J. Neurosci.* 30 (2010) 9292–9305.
- [9] C. Faivre-Sarrailh, F. Gauthier, N. Denisenko-Nehrbass, A. Le Bivic, G. Rougon, J.A. Girault, The glycosylphosphatidylinositol-anchored adhesion molecule F3/contactin is required for surface transport of paranodin/contactin-associated protein (caspr), *J. Cell Biol.* 149 (2000) 491–502.
- [10] S.H. Fatemi, A.R. Halt, G. Realmuto, J. Earle, D.A. Kist, P. Thuras, A. Merz, Purkinje cell size is reduced in cerebellum of patients with autism, *Cell Mol. Neurobiol.* 22 (2002) 171–175.
- [11] E. Fujita, H. Dai, Y. Tanabe, Y. Zhiling, T. Yamagata, T. Miyakawa, M. Tanokura, M.Y. Momoi, T. Momoi, Autism spectrum disorder is related to endoplasmic reticulum stress induced by mutations in the synaptic cell adhesion molecule, *CADM1, Cell Death Dis.* 1 (2010) e47.
- [12] E. Fujita, Y. Khoroku, K. Uruse, T. Tsukahara, M.Y. Momoi, H. Kumagai, T. Take-mura, T. Kuroki, T. Momoi, Involvement of Sonic hedgehog in the cell growth of LK-2 cells, human lung squamous carcinoma cells, *Biochem. Biophys. Res. Commun.* 238 (1997) 658–664.
- [13] E. Fujita, Y. Kuroku, S. Ozeki, Y. Tanabe, Y. Toyama, M. Maekawa, N. Kojima, H. Senoo, K. Toshimori, T. Momoi, Oligo-astheno-teratozoospermia in mice lacking RA175/TSLC1/SynCAM/IGSF4A, a cell adhesion molecule in the immunoglobulin superfamily, *Mol. Cell Biol.* 26 (2) (2006 Jan) 718–726.
- [14] E. Fujita, A. Soyama, T. Momoi, RA175, which is the mouse ortholog of TSLC1, a tumor suppressor gene in human lung cancer, is a cell adhesion molecule, *Exp. Cell Res.* 287 (2003) 57–66.
- [15] E. Fujita, Y. Tanabe, A. Shiota, M. Ueda, K. Suwa, M.Y. Momoi, T. Momoi, Ultrasonic vocalization impairment of Foxp2 (R552H) knockin mice related to speech-language disorder and abnormality of Purkinje cells, *Proc. Natl. Acad. Sci. U.S.A.* 105 (2008) 3117–3122.
- [16] S. Jamain, K. Radyushkin, K. Hammerschmidt, S. Granon, S. Boretius, F. Varoqueaux, N. Ramanantsoa, J. Gallego, A. Ronnenberg, D. Winter, J. Frahm, J. Fischer, T. Bourgeron, H. Ehrenreich, N. Brose, Reduced social interaction and ultrasonic communication in a mouse model of monogenic heritable autism, *Proc. Natl. Acad. Sci. U.S.A.* 105 (2008) 1705–1710.
- [17] C.S. Lai, S.E. Fisher, J.A. Hurst, F. Vargha-Khadem, A.P. Monaco, A forkhead-domain gene is mutated in a severe speech and language disorder, *Nature* 413 (2001) 519–523.
- [18] S. Li, J. Weidenfeld, E.E. Morrisey, Transcriptional and DNA binding activity of the Foxp1/2/4 family is modulated by heterotypic and homotypic protein interactions, *Mol. Cell Biol.* 24 (2004) 809–822.
- [19] T. Momoi, E. Fujita, H. Senoo, M. Momoi, Genetic factors and epigenetic factors for autism: endoplasmic reticulum stress and impaired synaptic function, *Cell Biol. Int.* 34 (2009) 13–19.
- [20] S. Oiso, Y. Takeda, T. Futagawa, T. Miura, S. Kuchiiwa, K. Nishida, R. Ikeda, H. Kariyazono, K. Watanabe, K. Yamada, Contactin-associated protein (Caspr) 2 interacts with carboxypeptidase E in the CNS, *J. Neurochem.* 109 (2009) 158–167.
- [21] E. Peles, J.L. Salzer, Molecular domains of myelinated axons, *Curr. Opin. Neurobiol.* 10 (2000) 558–565.
- [22] J. Pickett, E. London, The neuropathology of autism, *J. Neuropathol. Exp. Neurol.* 64 (2005) 925–935.
- [23] S. Poliak, L. Gollan, R. Martinez, A. Custer, S. Einheber, J.L. Salzer, J.S. Trimmer, P. Shrager, E. Peles, Caspr2, a new member of the neurexin superfamily, is localized at the juxtaparanodes of myelinated axons and associates with K⁺ channels, *Neuron* 24 (1999) 1037–1047.
- [24] W. Shu, J.Y. Cho, Y. Jiang, M. Zhang, D. Weisz, G.A. Elder, J. Schmeidler, R. De Gasperi, M.A. Sosa, D. Rabidou, A.C. Santucci, D. Perl, E. Morrisey, J.D. Buxbaum, Altered ultrasonic vocalization in mice with a disruption in the Foxp2 gene, *Proc. Natl. Acad. Sci. U.S.A.* 102 (2005) 9643–9648.
- [25] S.C. Vernes, D.F. Newbury, B.S. Abrahams, L. Winchester, J. Nicod, M. Groszer, M. Alarcón, P.L. Oliver, K.E. Davies, D.H. Geschwind, A.P. Monaco, S.E. Fisher, A functional genetic link between distinct developmental language disorders, *N. Engl. J. Med.* 359 (2008) 2337–2345.
- [26] Y. Zhiling, E. Fujita, Y. Tanabe, T. Yamagata, T. Momoi, M.Y. Momoi, Mutations in the gene encoding CADM1 are associated with autism spectrum disorder, *Biochem. Biophys. Res. Commun.* 377 (2008) 926–929.

ORIGINAL ARTICLE

Localisation of RA175 (Cadm1), a cell adhesion molecule of the immunoglobulin superfamily, in the mouse testis, and analysis of male infertility in the RA175-deficient mouse

M. Maekawa¹, C. Ito¹, Y. Toyama¹, F. Suzuki-Toyota¹, E. Fujita², T. Momoi² & K. Toshimori¹

¹ Department of Anatomy and Developmental Biology, Graduate School of Medicine, Chiba University, Chiba, Japan;

² Division of Differentiation and Development, Department of Inherited Metabolic Disorder, National Institute of Neuroscience, Tokyo, Japan

Keywords

Cadm1—immunoglobulin superfamily—infertility—spermatogenesis—testis

Correspondence

M. Maekawa, Department of Anatomy and Developmental Biology, Graduate School of Medicine, Chiba University, Chiba 260-8670, Japan.

Tel.: +81 43 226 2020;

Fax: +81 43 226 2021;

E-mail: mmaekawa@faculty.chiba-u.jp

Accepted: December 07, 2009

doi: 10.1111/j.1439-0272.2010.01049.x

Summary

RA175, a member of the immunoglobulin superfamily, plays an important role in cell adhesion, and RA175 gene-deficient mice (RA175^{-/-}) show oligoasthenoteratozoospermia. To understand the function of RA175, location in the testis and the morphological features of its spermatogenic cells in RA175^{-/-} mice were investigated. Immunohistochemical studies revealed that RA175 immunoreactivity was observed on the cell surface of the spermatogenic cells at specific stages. A strong reaction was detected from type A spermatogonia to pachytene spermatocytes at stage IV and from step 6 to step 16 spermatids during spermatogenesis. From pachytene spermatocytes at stage VI to step 4 spermatids, the reaction was not detected by the enzyme-labelled antibody method and was faintly detected by the indirect immunofluorescence method. Abnormal vacuoles in the seminiferous epithelium, showing exfoliation of germ cells, and ultrastructural abnormality of the elongate spermatids were revealed in the RA175^{-/-} testes. Other members of the immunoglobulin superfamily such as basigin, nectin-2 and nectin-3, which have an important role in spermatogenesis, were immunohistochemically detected in the RA175^{-/-} testis. These observations indicate a unique expression pattern of RA175 in the testis and provide clues regarding the mechanism of male infertility in the testis.

Introduction

Immunoglobulin superfamily (IgSF) molecules serve as cell adhesion receptors, and are implicated in diverse cellular phenomena such as cell shape and polarisation, cytoskeletal organisation, cell motility, proliferation, survival and differentiation (Holness & Simmons, 1994; Hynes, 1999). It is known that the IgSF members such as basigin and nectins are expressed in the testis and have a crucial function in spermatogenesis (Toshimori *et al.*, 2006). For example, basigin (CD147/EMMPRIN, Maekawa *et al.*, 1998; Toyama *et al.*, 1999), nectins (Bouchard *et al.*, 2000; Inagaki *et al.*, 2006) and Jam-C/Jam3 (Gliki *et al.*, 2004; Fujita *et al.*, 2007) are expressed on the testicular cells, and their gene-deficient mice show male sterility.

Another IgSF member, RA175 (Cadm1), was first characterised as one of the genes preferentially expressed during the differentiation of P19 mouse embryonal

carcinoma cells induced by retinoic acid (Urase *et al.*, 2001; Fujita *et al.*, 2003). The same molecule has been characterised independently and is called by different names: tumour suppressor of lung cancer 1 (TSLC1) (Kuramochi *et al.*, 2001); immunoglobulin superfamily member 4 (IGSF4) (Gomyo *et al.*, 1999); spermatogenic immunoglobulin superfamily member (SgIGSF) (Wakayama *et al.*, 2001); synaptic cell adhesion molecule (SynCAM) (Biederer *et al.*, 2002) and nectin-like molecule 2 (Nec12) (Shingai *et al.*, 2003). These facts indicate the diverse functions of the molecule RA175. RA175 has three immunoglobulin domains in its extracellular region that are involved in cell–cell adhesion via a homophilic or heterophilic interaction (Masuda *et al.*, 2002; Fujita *et al.*, 2003; Wakayama & Iseki, 2009). In order to elucidate the functions of RA175, we have generated mice lacking the gene and found that the resulting RA175^{-/-} male mice were infertile, showing oligoasthenoteratozoospermia

(Fujita *et al.*, 2006). *RA175*^{-/-} females and heterozygous mice were fertile and no obvious defects were observed. Mice deficient in this gene were subsequently reported by other groups (Surace *et al.*, 2006; van der Weyden *et al.*, 2006; Yamada *et al.*, 2006), and their results agreed with our previous report (Fujita *et al.*, 2006).

In this study, we investigated the location of RA175 in the testis in detail and the characteristics of *RA175*^{-/-} mice to understand the function of RA175. Furthermore, the location of other IgSF members, such as basigin, nectin-2 and nectin-3, which play important roles in spermatogenesis, was examined in the *RA175*^{-/-} testis.

Materials and methods

Animals and antibodies

The generation of mice with the targeted disruption of the *RA175* gene has been previously reported (Fujita *et al.*, 2006). Animal handling was approved by the Animal Research Committee of Chiba University. More than 10 *RA175*^{-/-} and *RA175*^{+/+} mice (3–6 months old) were examined in this study, and more than five sections were analysed per mouse by immunohistochemistry and indirect immunofluorescence. Anti-RA175 antibody was raised against a peptide corresponding to the C-terminal region of RA175, as described previously (Fujita *et al.*, 2003). Goat anti-basigin antibody (sc-9757) and goat anti-nectin-2 antibody (sc-14799) were purchased from Santa Cruz Biotechnology, Inc. (Santa Cruz, CA, USA), and rat monoclonal antibody against nectin-3 was obtained from Abcam (Cambridge, UK). The rat monoclonal antibody TRA98 was a gift from Dr Nishimune of Osaka University.

Immunohistochemistry

Wild-type mice were anaesthetised with pentobarbital and fixed with Bouin's fluid by perfusion through the left ventricle. Testes were removed, embedded in paraffin, and cut at a thickness of 3 μm . These sections were immunostained with either anti-RA175 antibody, anti-basigin antibody or anti-nectin-2 antibody. Non-specific binding of the antibody was blocked by placing the sections in phosphate buffered saline (PBS) containing 5% normal goat serum or foetal bovine serum for 30 min at room temperature (RT). The sections were then incubated with either rabbit anti-RA175 antibody, goat anti-basigin antibody or goat anti-nectin-2 antibody at 4 °C overnight. After washing with PBS, the samples were incubated with biotinylated goat anti-rabbit IgG (Dako Japan Company, Kyoto, Japan) or biotinylated rabbit anti-goat IgG (Dako) for 1 h, followed by incubation with streptavidin–biotin peroxidase complex solution (Dako) for 30 min.

Immunohistochemical reactions were visualised using 3,3'-diaminobenzidine and H₂O₂. Several adjacent sections were stained with periodic acid Schiff (PAS) and counterstained with haematoxylin to determine the stages of the seminiferous epithelium.

Indirect immunofluorescence (IIF)

Wild-type and *RA175*^{-/-} mice were anaesthetised with pentobarbital, and perfused through the heart with 4% paraformaldehyde in PBS. The testes and epididymides were removed and immersed in a fixative for an additional 4 h. They were embedded in OCT compound and cut at a thickness of 20 μm on a cryostat. After blocking the sections for 1 h at RT, the testicular sections were incubated with rabbit anti-RA175 antibody or rat anti-nectin-3 antibody, and the sections from the caput epididymidis were incubated with rat monoclonal antibody TRA98 at 4 °C overnight. The slides were then incubated with Alexa Fluor 488 goat anti-rabbit IgG (0.5 $\mu\text{g ml}^{-1}$; Invitrogen, Carlsbad, CA, USA) or goat anti-rat IgG (0.5 $\mu\text{g ml}^{-1}$; Invitrogen) together with propidium iodide (1 $\mu\text{g ml}^{-1}$; Sigma, St. Louis, MO, USA) and RNase (10 $\mu\text{g ml}^{-1}$; Sigma) in the blocking solution for 1 h at RT. After washing with PBS, the samples were mounted with PermaFluor (Immunon, Pittsburgh, PA, USA) and observed using a confocal laser scanning microscope (LSM510; Carl Zeiss, Oberkochen, Germany). To stain the actin filaments and nuclei in the testis, the frozen sections were incubated with 0.83 $\mu\text{g ml}^{-1}$ FITC-labelled phalloidin (Sigma), 1 $\mu\text{g ml}^{-1}$ propidium iodide (Sigma) and 10 $\mu\text{g ml}^{-1}$ RNase (Sigma) for 1 h, and observed under a confocal laser scanning microscope.

Transmission electron microscopy

The animals were anaesthetised with pentobarbital and perfused transcardially with 3% glutaraldehyde in HEPES buffer. The testes and epididymides were excised and immersed in the same fixative for 2 h at RT. After postfixation with 1% OsO₄, the tissues were embedded in epoxy resin. Ultrathin sections were prepared, stained with uranyl acetate and lead citrate, and observed under an electron microscope (JEM 1200EX, JEOL, Tokyo, Japan).

Results

Immunohistochemical localisation of RA175 in the mouse testis

The immunohistochemical localisation of RA175 in the wild-type mouse testis was determined by the enzyme-labelled antibody method (Fig. 1). Paraffin sections of the

testis were immunostained with rabbit anti-RA175 antibody. Adjacent sections were stained with PAS and haematoxylin to identify the stages of the seminiferous tubules (data not shown). The results revealed the stage-specific localisation of RA175 in the testicular germ cells. RA175 immunoreactivity was detected on the cell surface of spermatogonia and spermatocytes until stage IV, although all type A spermatogonia did not exhibit a positive reaction. The immunoreactivity became weak in the pachytene spermatocytes at stage V and was not detected in the pachytene spermatocytes at stage VI through step 4 round spermatids at stage IV. Interestingly, the positive staining reappeared on the cell surface of step 5 spermatids. Staining around the head became weak in step 13 spermatids and then disappeared in step 14 spermatids, whereas immunoreactivity around the cytoplasm was detected. Just before spermiation, immunoreactivity was detected only in the residual bodies. Mature sperm in the cauda

epididymidis did not exhibit an immunopositive reaction (data not shown). A detailed examination revealed that the immunopositive reaction was confined to the apical surface of type A spermatogonia and was not detected in the basal surface which is in contact with the basal lamina (Fig. 1g). These results are summarised in Fig. 1h. Control experiments using *RA175*^{-/-} testes revealed no RA175 immunoreaction in the spermatogenic cells.

Localisation of RA175 in the testis detected by IIF

Localisation of RA175 in the testis was also detected by IIF (Fig. 2), and positive reactions were observed in the germ cells within the seminiferous tubules. Germ cells immunostained by the enzyme-labelled antibody method (Fig. 1) were also IIF positive (Fig. 2). In addition, late pachytene spermatocytes to early round spermatids, which did not show a positive reaction by the

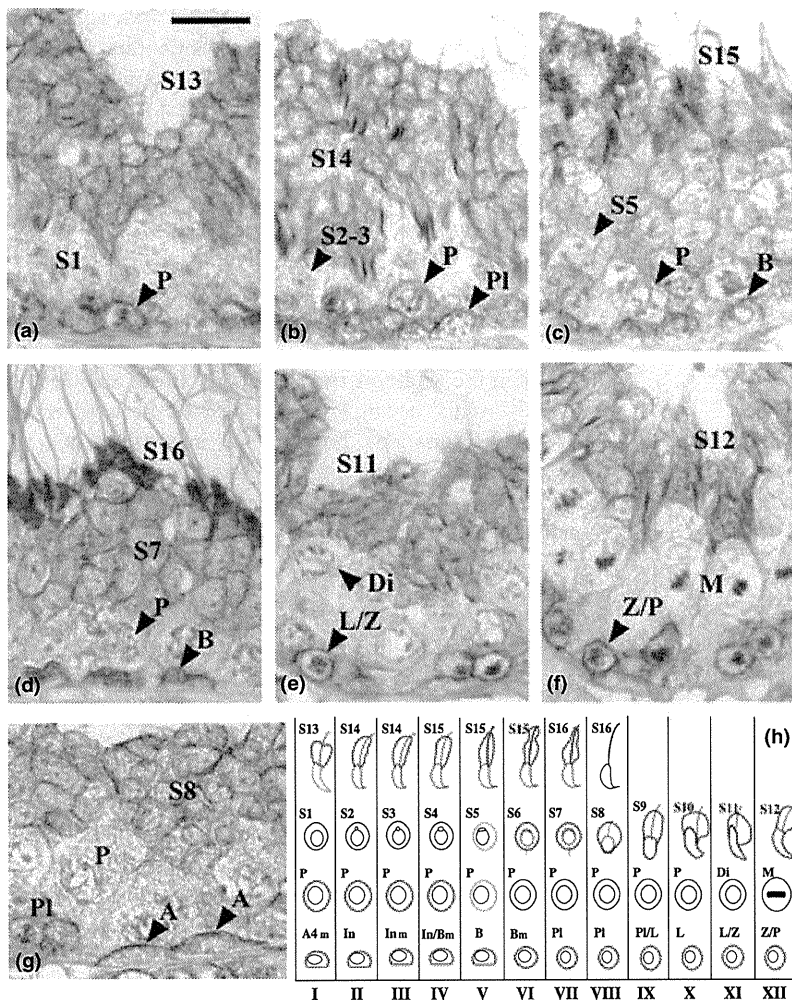


Fig. 1 Immunohistochemical localisation of RA175 in the mouse seminiferous epithelium. (a-g) Paraffin sections of wild-type mouse testes were immunostained with an anti-RA175 antibody (brown) by the enzyme-labelled antibody method and were counterstained with haematoxylin (blue). (a) Stage I, (b) Stage II-III, (c) Stage V, (d) Stage VII, (e) Stage XI, (f) Stage XII. (g) Stage VIII. Bar = 20 μ m. (h) Summary of the immunolocalisation of RA175 in the testis. Positive immunostaining is shown in red. A, type A spermatogonia; B, type B spermatogonia; Pl, preleptotene spermatocyte; LZ, leptotene/zygotene spermatocyte; Z/P, zygotene/pachytene spermatocyte; P, pachytene spermatocyte; Di, diplotene spermatocyte; M, metaphase of the spermatocyte; S1, S2-3, S5, S7, S8, S11, S13, S14, S15 and S16, step 1, 2-3, 5, 7, 8, 11, 13, 14, 15 and 16 spermatid respectively.

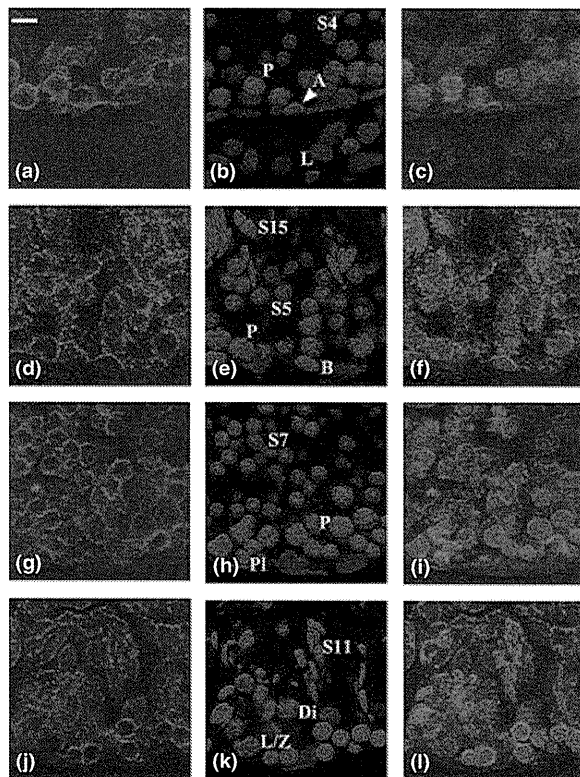


Fig. 2 Immunolocalisation of RA175 in the mouse seminiferous epithelium revealed by IIF. Frozen sections of wild-type testes were immunostained with anti-RA175 antibody (green; a, d, g) and counterstained with propidium iodide for nuclei (red; b, e, h). c, f and l shows merged images. (a–c) Stage IV, (d–f) stage V, (g–i) stage VII, (j–l) stage XI. Bar = 10 μ m.

enzyme-labelled antibody method (Fig. 1), were found to be IIF positive. Although reactivity on the cell surface was less distinctive, a diffuse staining in the cytoplasm was revealed by IIF staining (Fig. 2).

Morphological characterisation of the testis and epididymis from *RA175*^{-/-} mouse

Testes from *RA175*^{-/-} mice frequently exhibited abnormal vacuoles in the seminiferous epithelium (Fig. 3a, b). Elongate spermatids were obviously reduced in number in the *RA175*^{-/-} testis. Electron micrographs revealed elongate spermatids with deformed nuclei and/or acrosomes, which were observed frequently in the *RA175*^{-/-} testis (Fig. 3e). An ectopic manchette (Fig. 3f) was often observed; 16 spermatids had irregular manchette out of 44 spermatids. Although the marginal rings of the acroplaxome appeared normal (Fig. 3g), apical ectoplasmic specialisations of the Sertoli cells were separated from the

spermatids, and small vacuoles were formed around the spermatids (Fig. 3g, h). This is probably caused by the dissociation of the elongate spermatids from the Sertoli cells through lack of RA175.

Many cells, but not spermatozoa, were found in the epididymis of the *RA175*^{-/-} mouse (Fig. 4). An indirect immunofluorescence study using TRA98 revealed that many cells in the epididymal duct were immunopositive. As the TRA98 antibody recognises germ cells at various stages of differentiation from spermatogonia to spermatids (Tanaka *et al.*, 1997), the positive cells were identified as immature spermatogenic cells and not as spermatozoa (Fig. 4b, d). Round spermatids such as step 3, 5 and 7 spermatids were detected in the epididymal duct by electron microscopy (Fig. 4e, f).

Localisation of basigin, nectin-2 and nectin-3 in the *RA175*^{-/-} testis

To examine the expression of other IgSF members, testes from *RA175*^{-/-} mice were immunostained with anti-basigin, anti-nectin-2 and anti-nectin-3 antibodies (Fig. 5). Basigin was detected in the cytoplasm of round spermatids as well as in the periphery of spermatocytes and spermatids in the wild-type testes (Fig. 5b). In the *RA175*^{-/-} testes, the localisation of basigin was similar to that in the wild-type testes (Fig. 5a). Nectin-2 was localised at the ectoplasmic specialisations of the Sertoli cells, which locates both in the Sertoli–Sertoli junctions of the basal regions (basal ectoplasmic specialisation) and in the Sertoli–spermatid junctions of the adluminal regions (apical ectoplasmic specialisation) of the seminiferous tubules in the wild-type testes (Fig. 5d). In the case of the *RA175*^{-/-} testis, nectin-2 was detected at the basal ectoplasmic specialisations, however, the immunoreaction at the apical ectoplasmic specialisations was not conspicuous, partly because the number of normal elongate spermatids was considerably decreased (Fig. 5c). Nectin-3 was localised in the spermatids adjoining the apical ectoplasmic specialisations in the wild-type testis (Fig. 5f). The spermatids at step 8–9 in the *RA175*^{-/-} testis exhibited a similar nectin-3-immunopositive reaction to the wild-type testis (data not shown). However, at stage XII, when the abnormal morphology of the elongate spermatids at step 12 became noticeable in the *RA175*^{-/-} testis, nectin-3 immunoreactivity was reduced in comparison with that in the wild-type testis (Fig. 5e, f).

An abnormal distribution of actin filaments in the *RA175*^{-/-} testis was revealed by phalloidin staining (Fig. 5g, h). Actin filaments were not observed around the malformed heads of elongate spermatids, and an accumulation of the actin filaments was found in the seminiferous tubules.

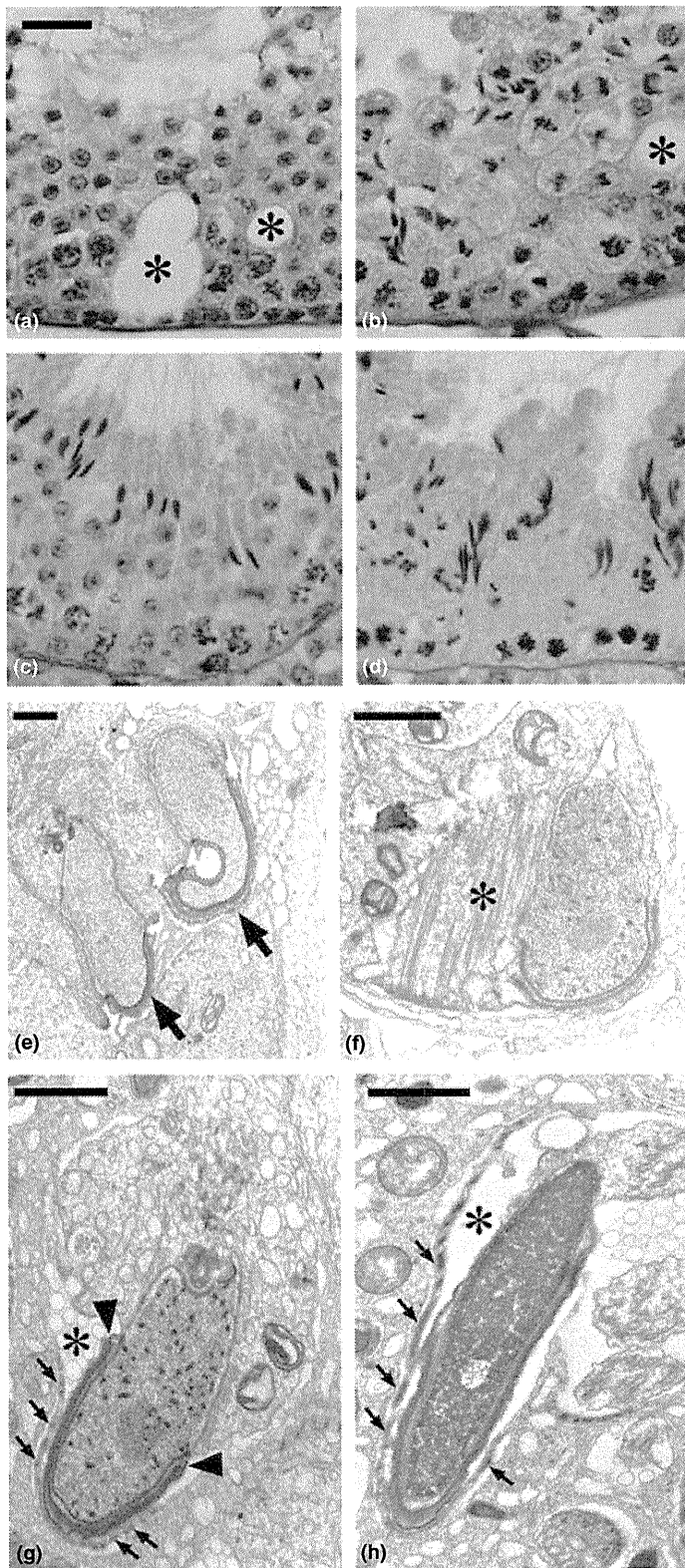


Fig. 3 (a–d) Seminiferous epithelia at stage VI (a, c) and XII (b, d) from *RA175*^{-/-} (a, b) and wild-type mice (c, d) stained with PAS-haematoxylin. The number of elongate spermatids was markedly decreased and vacuoles (*) in the seminiferous tubules were observed in the *RA175*^{-/-} testes (a, b). Bar = 20 μ m. (e–h) Electron microphotographs of *RA175*^{-/-} testis. Step 9 spermatids with deformed nuclei and acrosomes (e; arrows) and with ectopic manchette (f; asterisk). Small vacuoles (g; asterisk) and dissociation (h; asterisk) between the acrosome of the spermatid and ectoplasmic specialisation (g, h; small arrows) in the Sertoli cell are observed. The marginal rings of the acroplaxome (g; arrowheads) appear to be normal. Bar = 1 μ m.

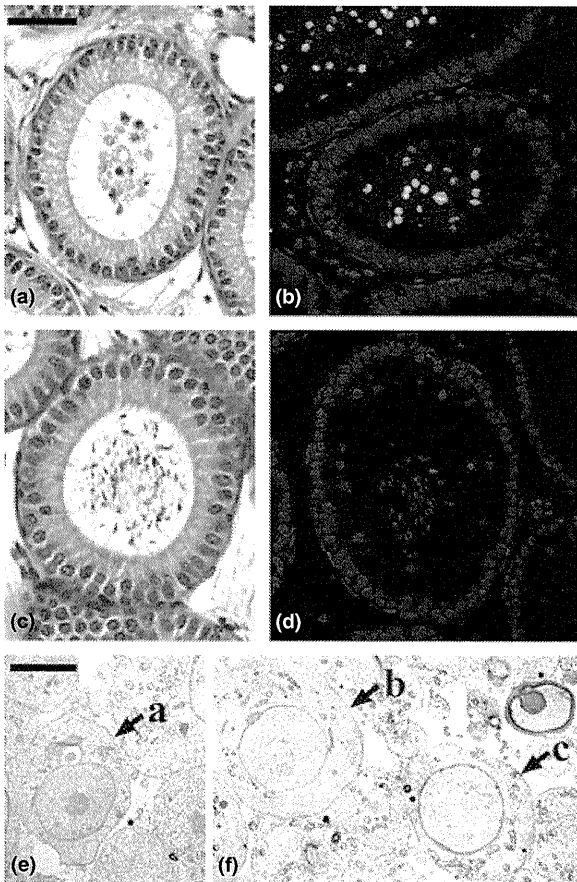


Fig. 4 Caput epididymidis from *RA175*^{-/-} (a, b, e, f) and wild-type mice (c, d). (a, c) Stained with haematoxylin and eosin. (b, d) Immunostained with TRA98 antibody (green) and propidium iodide (red). Bar = 50 μ m. (e, f) Electron micrographs of the lumen of the caput epididymidis from *RA175*^{-/-} mouse. Step 3 (a), step 5 (b) and step 7 (c) spermatids were observed in the lumen. Bar = 5 μ m.

Discussion

To clarify the function of RA175 during spermatogenesis, it is essential to detect the precise location of this molecule in the testis. Our results in this report (Fig. 1h) revealed a few differences from the previous study (Wakayama *et al.*, 2003; Yamada *et al.*, 2006), which reported that the RA175 protein was detected in spermatogenic cells from intermediate spermatogonia to early pachytene spermatocytes and from step 7 spermatids to the residual bodies of step 16 spermatids. First, we found that several type A spermatogonia were immunopositive for RA175. Spermatogonia are classified either as type A, intermediate, or type B. Type A spermatogonia are the most primitive spermatogonia and are subdivided into undifferentiated (As, Apr and Aal) and differentiating (A1,

A2, A3 and A4) spermatogonia (de Rooij & Grootegoed, 1998). As immunonegative type A spermatogonia were also detected, all subpopulations of type A spermatogonia do not express RA175. At present, it is not yet known which subtype(s) of type A spermatogonia express the RA175 protein, however, RA175 can be used as a marker for the differentiation of type A spermatogonia. Secondly, we found RA175 immunoreactivity until pachytene spermatocytes at stage IV, and the reaction diminished thereafter and was not detected from pachytene spermatocytes at stage IV through step 4 spermatids. Subsequently, the activity reappeared in step 5–6 spermatids. Furthermore, by the IIF method, positive reactions for RA175 were detected to some extent in the cytoplasm of mid- to late-pachytene spermatocytes and in round spermatids, which showed no positive staining by the enzyme-labelled antibody method. These differences might be caused by the experimental systems, including the mice strains and antibodies used. However, our IIF results might reflect the intrinsic distribution of RA175, which does not completely disappear during the mid-pachytene spermatocyte to the step 4 spermatid stage.

RA175 immunoreactivity was found at the apical site and not at the basal site of the spermatogonia. This implies that RA175 is localised at the germ cell surface which contacts the Sertoli cells. Thus, it is important to detect the binding partner of RA175 which probably exists in the Sertoli cells. Wakayama *et al.* (2007) identified a poliovirus receptor (PVR) as a binding partner of RA175, which was present in the Sertoli cells of the mouse testis. This finding implies a heterophilic binding between RA175 on germ cells and PVR on the Sertoli cells in the testis.

In *RA175*^{-/-} mice, the number of elongate spermatids was remarkably decreased in the testes, and the remaining elongate spermatids had abnormally shaped heads and acrosomes. Vacuoles were frequently found in the seminiferous epithelium of the *RA175*^{-/-} testis, implying that a cluster of germ cells was exfoliated from the seminiferous epithelium. These observations agreed with those of previous reports (Fujita *et al.*, 2006; van der Weyden *et al.*, 2006; Yamada *et al.*, 2006) and demonstrated that RA175 is responsible for the attachment of germ cells to the seminiferous epithelium and spermatid morphogenesis in the testis. The exfoliated germ cells are partly phagocytosed by Sertoli cells (Fujita *et al.*, 2006), and other cells accumulate in the epididymal duct. It is notable that all germ cells showing RA175-immunopositive reaction were not necessarily exfoliated from the seminiferous epithelium in the *RA175*^{-/-} testis. Other factors probably compensate in part for the function of RA175. Basigin, another IgSF member, exists in these germ cell stages. The molecule was also detected in the

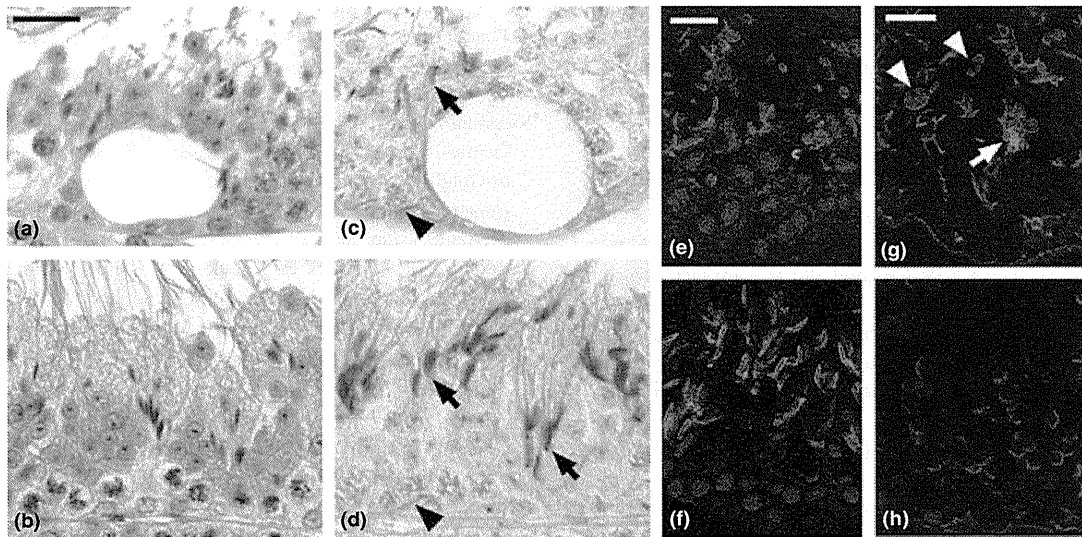


Fig. 5 Immunohistochemical localisation of basigin (a, b), nectin-2 (c, d) and nectin-3 (e, f), and distribution of actin filaments (g, h) in the testis. Testes from *RA175*^{-/-} (a, c, e, g) and wild-type mice (b, d, f, h) were stained with anti-basigin antibody (a, b), anti-nectin-2 antibody (c, d), anti-nectin-3 antibody (e, f), or FITC-labelled phalloidin (g, h), and counterstained with haematoxylin (a–d) or propidium iodide (red; e–h). Arrowheads in (c), (d); basal ectoplasmic specialisations. Arrows in (c), (d); apical ectoplasmic specialisations. (g, h) In the *RA175*^{-/-} testes, actin filaments were not observed around the malformed head of the elongate spermatids (arrowheads in g), and were observed to accumulate in the seminiferous tubules (arrow in g). Bar = 20 µm.

RA175^{-/-} testis and is one of the candidates for such factors.

An ultrastructural investigation of elongate spermatids in the *RA175*^{-/-} testis demonstrated abnormal morphology of the manchette, a microtubular structure around the nucleus of the elongate spermatid. The ectopic manchette of the spermatid has been reported in other gene-deficient mice showing male infertility, such as *GOPC*^{-/-} (Ito *et al.*, 2004) and *Hrb*^{-/-} (Kierszenbaum *et al.*, 2004) mice. The manchette is involved in the nuclear elongation and condensation of the spermatid, and spermatozoa from *GOPC*^{-/-} and *Hrb*^{-/-} mice have round heads without acrosomes, which are different from the *RA175*^{-/-} phenotype. Another structure termed the acroplaxome, an F-actin/keratin 5-containing cytoskeletal plate anchored to the spermatid nucleus (Kierszenbaum *et al.*, 2003), is also important in determining the shape of the spermatid head. The acroplaxomes appeared to be normal in *RA175*^{-/-} mice, and the abnormal shapes of the heads and acrosomes of the elongate spermatids in the *RA175*^{-/-} testis were not triggered by the acroplaxome abnormality, and could be a secondary effect of *RA175* deficiency.

An unusual accumulation of actin filaments near the lumen of the seminiferous tubules was observed in the *RA175*^{-/-} testis. These actin filaments were components of the apical ectoplasmic specialisations between Sertoli cells and spermatids, and were formed from the discarded

ectoplasmic specialisations of exfoliated spermatids. Such structures are frequently found in seminiferous tubules lacking spermatids (Hosoi *et al.*, 2002).

Nectin-2 and nectin-3 are associated with the actin cytoskeleton through afadin, and nectin-2 on Sertoli cells and nectin-3 on spermatids interact at the apical ectoplasmic specialisations (Ozaki-Kuroda *et al.*, 2002). We examined the immunolocalisation of nectin-2 and nectin-3 in the *RA175*^{-/-} testis, and their signals were decreased or lost around the malformed heads of the elongate spermatids, indicating the detachment of spermatids from the Sertoli cells in the seminiferous epithelium. However, a small number of elongate spermatids that survived and appeared to have normal morphology showed positive immunoreactions for nectins. Although nectin-3 is reported to interact with RA175 (*necl-2*) (Takai *et al.*, 2003), their expression sites were differed in the testis, and the roles of RA175 and nectins are different in spermatogenesis as discussed in the previous paper (Fujita *et al.*, 2006).

In this report, we revealed the characteristic pattern of RA175 expression in the testis, and demonstrated that basigin, nectin-2 and nectin-3, the other members of IgSF, were also expressed in the *RA175*^{-/-} testis. Many IgSF members are necessary to achieve normal spermatogenesis in the testis, and RA175 plays an important role as an adherent molecule between the germ cells and Sertoli cells in the testis. Further studies will provide

important clues regarding the regulation of the mechanism of the cell adhesion system in the testis and in understanding human infertility.

References

- Biederer T, Sara Y, Mozhayeva M, Atasoy D, Liu X, Kavalali ET, Sudhof TC (2002) SynCAM, a synaptic adhesion molecule that drives synapse assembly. *Science* 297:1525–1531.
- Bouchard MJ, Dong Y, McDermott BM Jr, Lam DH, Brown KR, Shelanski M, Bellve AR, Racaniello VR (2000) Defects in nuclear and cytoskeletal morphology and mitochondrial localization in spermatozoa of mice lacking nectin-2, a component of cell-cell adherens junctions. *Mol Cell Biol* 20:2865–2873.
- Fujita E, Soyama A, Momoi T (2003) RA175, which is the mouse ortholog of TSLC1, a tumor suppressor gene in human lung cancer, is a cell adhesion molecule. *Exp Cell Res* 287:57–66.
- Fujita E, Kouroku Y, Ozeki S, Tanabe Y, Toyama Y, Maekawa M, Kojima N, Senoo H, Toshimori K, Momoi T (2006) Oligo-astheno-teratozoospermia in mice lacking RA175/TSLC1/SynCAM/IGSF4A, a cell adhesion molecule in the immunoglobulin superfamily. *Mol Cell Biol* 26:718–726.
- Fujita E, Tanabe Y, Hirose T, Aurrand-Lions M, Kasahara T, Imhof BA, Ohno S, Momoi T (2007) Loss of partitioning-defective-3/isotype-specific interacting protein (par-3/ASIP) in the elongating spermatid of RA175 (IGSF4A/SynCAM)-deficient mice. *Am J Pathol* 171:1800–1810.
- Gliki G, Ebnet K, Aurrand-Lions M, Imhof BA, Adams RH (2004) Spermatid differentiation requires the assembly of a cell polarity complex downstream of junctional adhesion molecule-C. *Nature* 431:320–324.
- Gomyo H, Arai Y, Tanigami A, Murakami Y, Hattori M, Hosoda F, Arai K, Aikawa Y, Tsuda H, Hirohashi S, Asakawa S, Shimizu N, Soeda E, Sakaki Y, Ohki M (1999) A 2-Mb sequence-ready contig map and a novel immunoglobulin superfamily gene IGSF4 in the LOH region of chromosome 11q23.2. *Genomics* 62:139–146.
- Holness CL, Simmons DL (1994) Structural motifs for recognition and adhesion in members of the immunoglobulin superfamily. *J Cell Sci* 107(Pt 8):2065–2070.
- Hosoi I, Toyama Y, Maekawa M, Ito H, Yuasa S (2002) Development of the blood-testis barrier in the mouse is delayed by neonatally administered diethylstilbestrol but not by beta-estradiol 3-benzoate. *Andrologia* 34:255–262.
- Hynes RO (1999) Cell adhesion: old and new questions. *Trends Cell Biol* 9:M33–M37.
- Inagaki M, Irie K, Ishizaki H, Tanaka-Okamoto M, Miyoshi J, Takai Y (2006) Role of cell adhesion molecule nectin-3 in spermatid development. *Genes Cells* 11:1125–1132.
- Ito C, Suzuki-Toyota F, Maekawa M, Toyama Y, Yao R, Noda T, Toshimori K (2004) Failure to assemble the peri-nuclear structures in GOPC deficient spermatids as found in round-headed spermatozoa. *Arch Histol Cytol* 67:349–360.
- Kierszenbaum AL, Rivkin E, Tres LL (2003) Acroplaxome, an F-actin-keratin-containing plate, anchors the acrosome to the nucleus during shaping of the spermatid head. *Mol Biol Cell* 14:4628–4640.
- Kierszenbaum AL, Tres LL, Rivkin E, Kang-Decker N, van Deursen JM (2004) The acroplaxome is the docking site of Golgi-derived myosin Va/Rab27a/b-containing proacrosomal vesicles in wild-type and Hrb mutant mouse spermatids. *Biol Reprod* 70:1400–1410.
- Kuramochi M, Fukuhara H, Nobukuni T, Kanbe T, Maruyama T, Ghosh HP, Pletcher M, Isomura M, Onizuka M, Kitamura T, Sekiya T, Reeves RH, Murakami Y (2001) TSLC1 is a tumor-suppressor gene in human non-small-cell lung cancer. *Nat Genet* 27:427–430.
- Maekawa M, Suzuki-Toyota F, Toyama Y, Kadomatsu K, Hagihara M, Kuno N, Muramatsu T, Dohmae K, Yuasa S (1998) Stage-specific localization of basigin, a member of the immunoglobulin superfamily, during mouse spermatogenesis. *Arch Histol Cytol* 61:405–415.
- Masuda M, Yageta M, Fukuhara H, Kuramochi M, Maruyama T, Nomoto A, Murakami Y (2002) The tumor suppressor protein TSLC1 is involved in cell-cell adhesion. *J Biol Chem* 277:31014–31019.
- Ozaki-Kuroda K, Nakanishi H, Ohta H, Tanaka H, Kurihara H, Mueller S, Irie K, Ikeda W, Sakai T, Wimmer E, Nishimune Y, Takai Y (2002) Nectin couples cell-cell adhesion and the actin scaffold at heterotypic testicular junctions. *Curr Biol* 12:1145–1150.
- de Rooij DG, Grootegoed JA (1998) Spermatogonial stem cells. *Curr Opin Cell Biol* 10:694–701.
- Shingai T, Ikeda W, Kakunaga S, Morimoto K, Takekuni K, Itoh S, Satoh K, Takeuchi M, Imai T, Monden M, Takai Y (2003) Implications of nectin-like molecule-2/IGSF4/RA175/SgIGSF/TSLC1/SynCAM1 in cell-cell adhesion and transmembrane protein localization in epithelial cells. *J Biol Chem* 278:35421–35427.
- Surace EI, Strickland A, Hess RA, Gutmann DH, Naughton CK (2006) Tslc1 (nectin-like molecule-2) is essential for spermatozoa motility and male fertility. *J Androl* 27:816–825.
- Takai Y, Irie K, Shimizu K, Sakisaka T, Ikeda W (2003) Nectins and nectin-like molecules: roles in cell adhesion, migration, and polarization. *Cancer Sci* 94:655–667.
- Tanaka H, Pereira LA, Nozaki M, Tsuchida J, Sawada K, Mori H, Nishimune Y (1997) A germ cell-specific nuclear antigen recognized by a monoclonal antibody raised against mouse testicular germ cells. *Int J Androl* 20:361–366.
- Toshimori K, Maekawa M, Ito C, Toyama Y, Suzuki-Toyota F, Saxena D (2006) The involvement of immunoglobulin superfamily proteins in spermatogenesis and sperm-egg interaction. *Reprod Med Biol* 5:87–93.
- Toyama Y, Maekawa M, Kadomatsu K, Miyauchi T, Muramatsu T, Yuasa S (1999) Histological characterization of defective spermatogenesis in mice lacking the basigin gene. *Anat Histol Embryol* 28:205–213.

- Urase K, Soyama A, Fujita E, Momoi T (2001) Expression of RA175 mRNA, a new member of the immunoglobulin superfamily, in developing mouse brain. *Neuroreport* 12:3217–3221.
- Wakayama T, Iseki S (2009) Role of the spermatogenic-Sertoli cell interaction through cell adhesion molecule-1 (CADM1) in spermatogenesis. *Anat Sci Int* 84:112–121.
- Wakayama T, Ohashi K, Mizuno K, Iseki S (2001) Cloning and characterization of a novel mouse immunoglobulin superfamily gene expressed in early spermatogenic cells. *Mol Reprod Dev* 60:158–164.
- Wakayama T, Koami H, Ariga H, Kobayashi D, Sai Y, Tsuji A, Yamamoto M, Iseki S (2003) Expression and functional characterization of the adhesion molecule spermatogenic immunoglobulin superfamily in the mouse testis. *Biol Reprod* 68:1755–1763.
- Wakayama T, Sai Y, Ito A, Kato Y, Kurobo M, Murakami Y, Nakashima E, Tsuji A, Kitamura Y, Iseki S (2007) Heterophilic binding of the adhesion molecules poliovirus receptor and immunoglobulin superfamily 4A in the interaction between mouse spermatogenic and Sertoli cells. *Biol Reprod* 76:1081–1090.
- van der Weyden L, Arends MJ, Chausiaux OE, Ellis PJ, Lange UC, Surani MA, Affara N, Murakami Y, Adams DJ, Bradley A (2006) Loss of TSLC1 causes male infertility due to a defect at the spermatid stage of spermatogenesis. *Mol Cell Biol* 26:3595–3609.
- Yamada D, Yoshida M, Williams YN, Fukami T, Kikuchi S, Masuda M, Maruyama T, Ohta T, Nakae D, Maekawa A, Kitamura T, Murakami Y (2006) Disruption of spermatogenic cell adhesion and male infertility in mice lacking TSLC1/IGSF4, an immunoglobulin superfamily cell adhesion molecule. *Mol Cell Biol* 26:3610–3624.

